Geochemical Perspectives Letters

Global patterns of radiocarbon depletion in subsoil linked to rock-derived organic carbon

K.E. Grant[1,2*], R.G. Hilton[3], V.V. Galy[4]

OPEN ACCESS

https://doi.org/10.7185/geochemlet.2312

Abstract

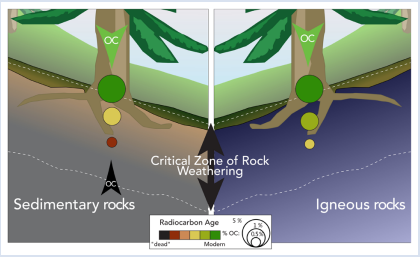

Organic matter stored in sedimentary rocks is one of the largest stocks of carbon at Earth's surface. The fate of this rock organic carbon (OC_{petro}) during weathering in soils influences the geological carbon cycle, and impacts soil radiocarbon content that is used to quantify soil carbon turnover. Here, we assess the potential contribution of OC_{petro} to soils, using a mixing model generated by a global dataset of soil radiocarbon measurements (^{14}C). Soils developed on sedimentary rocks (rather than on igneous substrate) have a paired OC content and ^{14}C values consistent with OC_{petro} input, giving rise to apparent increase in soil residence time. We call for renewed assessment of OC_{petro} input to soils, in terms of its impact on soil radiocarbon inventories, and its potential to release carbon dioxide.

Received 23 June 2022 | Accepted 6 March 2023 | Published 19 April 2023

Introduction

Sedimentary rocks cover 64 % of Earth's surface (Hartmann and Moosdorf, 2012). Within the upper 1 m, there are an estimated 1100 petagrams of carbon (PgC) present as radiocarbon (^{14}C) "dead" rock organic carbon (OC_{petro}) (Copard *et al.*, 2007), equivalent to the carbon stock in soils derived from the biosphere (Jackson *et al.*, 2017). When soil forms on sedimentary rocks, OC_{petro} is a "bottom up" input of carbon that can contribute to the soil OC pool, especially in deep soils with low OC concentrations (Hemingway *et al.*, 2018; Kalks *et al.*, 2021). While OC_{petro} could be widespread in soils developed on sedimentary rocks, observations come from only a handful of weathering profiles, including OC_{petro}-rich rocks, such as black shales which are not globally representative (Petsch *et al.*, 2001). In addition, estimates of global OC_{petro} surface exposure are based on upscaling from geological maps (Copard *et al.*, 2007), but this input has not been assessed in soil carbon studies. While there is widespread evidence for OC_{petro} in sediments from rivers around the world (*e.g.*, Galy *et al.*, 2015; Clarke *et al.*, 2017), we lack constraint on the input of OC_{petro} to soils.

Input of OC_{petro} to soil is important for two reasons. First, the exposure of rocks to weathering can drive OC_{petro} oxidation, releasing CO_2 and consuming O_2, with global emissions of CO_2 from OC_{petro} oxidation similar to those from volcanism (Petsch, 2014; Hilton and West, 2020). Second, OC_{petro} input can increase the mean age of soil OC based on radiocarbon (Agnelli *et al.*, 2002), used to quantify atmospheric CO_2 exchange by (Trumbore, 2000; Shi *et al.*, 2020). Soils slow the rapid degradation of "modern" plant-derived vegetation (OC_{bio}) through mineral and physical interactions, helping store OC_{bio} in soils over decades to millennia (Shi *et al.*, 2020). In the topsoil, the OC pool is dominated by plant and microbial organic matter and is generally ^{14}C-enriched (Shi *et al.*, 2020). In deeper soils (~>30 cm), recent studies (Mathieu *et al.*, 2015; He *et al.*, 2016; Shi *et al.*, 2020) show that ^{14}C-depleted ("old") OC is common around the world. These studies attribute "old" ^{14}C ages to an increase in OC-mineral interactions, as the clay content and mineral to organic ratio increase with depth and mineral surfaces can reduce the bioavailability and thus increase the persistence of OC_{bio} (Schmidt *et al.*, 2011). Soil C age distributions can have very long tails, with a small amount of old or ^{14}C-dead C skewing the mean age (Sierra *et al.*, 2018). However, inputs of ^{14}C-dead OC_{petro} are not considered in He *et al.* (2016) and Shi *et al.* (2020), despite the recognition that OC_{petro} inputs result in an "apparent" ageing of soil OC_{bio}.

Here, we quantify OC_{petro} in globally distributed soil profiles using the International Soil Radiocarbon Database (ISRaD database, see Supplementary Information) (Lawrence *et al.*, 2020). We separate soil profiles developed on igneous rocks (IG: negligible OC_{petro}) *versus* sedimentary rocks (SED: potential OC_{petro} inputs) using global geological maps and compare bulk ^{14}C signatures and % OC distributions. Alongside the global data set, using a mixing model analysis, we compare measurements made on river and soil OC in settings where OC_{petro} inputs have been demonstrated and where OC_{petro} is absent. Together, we assess the contribution of OC_{petro} to deep soils around the world and the implications for soil radiocarbon inventories and the surface carbon cycle.

1. Department of Geography, Durham University, South Road, Durham, DH1 3LE, UK
2. Center for Accelerator Mass Spectrometry, Lawrence Livermore National Laboratory, 7000 East Ave, Livermore, CA 94550, USA
3. Department of Earth Sciences, University of Oxford, South Parks Rd, Oxford, OX1 3AN, UK
4. Department of Marine Chemistry and Geochemistry, Woods Hole Oceanographic Institution, 266 Woods Hole Road, Woods Hole, MA 02543, USA
* Corresponding author (email: grant39@llnl.gov)

Evidence of OC_{petro} in soils and rivers using mixing models

The ^{14}C-depletion of soil OC can result from both: (1) ageing of OC_{bio} from plant and microbial derived material, stabilised by physical/chemical protection or intrinsic refractory properties (Hemingway *et al.*, 2019); and (2) mixing of OC_{petro} from rocks (^{14}C-free relative to instrumental background) with OC_{bio} (Petsch *et al.*, 2001; Hemingway *et al.*, 2018). To explore these scenarios, we examine cases where OC_{petro} contributes to bulk OC in river sediment loads and soils, with OC_{petro} inputs identified from geochemical proxies other than bulk ^{14}C (*e.g.*, C/N, $\delta^{13}C$, biomarkers, Raman spectroscopy, Ramped Pyrolysis Oxidation-^{14}C). These can be compared to examples where OC_{petro} inputs are absent and OC_{bio} decay/ageing acts alone from river sediments and soils on igneous bedrock (Fig. 1a, c). We find a notable contrast in the relationship between 1/[OC] and $\Delta^{14}C$ in sedimentary and igneous bedrock settings. Patterns expected for mixing between OC_{petro} and OC_{bio} appear to dominate in sedimentary settings.

An Andean Mountain river draining shales (Clark *et al.*, 2017) has river sediment OC $\Delta^{14}C$ values that ranged from −0.5 ‰ to −839 ‰. Clark *et al.* (2017) concluded that, on average, 0.37 ± 0.03 % of the suspended sediment mass was OC_{petro}. There is a significant linear trend between $\Delta^{14}C$ values and 1/[OC] ($p < 0.05$, $R^2 = 0.75$, Fig. 1a) that was attributed to binary mixing of OC_{petro} and biospheric OC supplied by erosion processes. In Himalayan rivers, the river OC also has a linear relationship between these variables ($p < 0.05$, $R^2 = 0.37$), albeit with a shallower slope due to lower OC_{petro} contents (Galy *et al.*, 2015). In soils, OC_{petro} has been recognised in only a few studies (Petsch, 2014; Hemingway *et al.*, 2018; Hilton *et al.*, 2021; Kalks *et al.*, 2021). In Taiwan, high erosion rates continuously supply fresh bedrock to the surface and keep surface soils young, and these samples have a linear relationship between $\Delta^{14}C$ and 1/[OC]. Mixing models show that OC_{petro} input to sediments and soils result in a linear trend between 1/[OC] and $\Delta^{14}C$ (Supplementary Information, Eq. S-8; Fig. 1b). These can explain the main patterns seen in the Andes and Himalayan rivers and Taiwanese soil data.

In contrast to the river sediments draining sedimentary rocks, rivers from a basaltic catchment, the Efri Haukadalsá River in Iceland (Torres *et al.*, 2020), have ^{14}C value ranging from −60 ‰ to −395 ‰ and display no relationship between 1/[OC] and $\Delta^{14}C$ (Fig. 1c). Torres *et al.* (2020) attributed the ^{14}C-depletion to erosion of millennial-aged OC from soils. In tropical soils, formed along a climate gradient underlain by a 450 ka lava flow from Hawaii, [OC] remains high while OC ages due to Fe-oxide mineral-carbon stabilisation, and these materials have an almost vertical array in 1/[OC] and $\Delta^{14}C$ (Fig. 1c; Grant *et al.*, 2022). These patterns in the data are more consistent with the paired evolution of 1/[OC] and $\Delta^{14}C$ expected for OC loss and ageing of OC, explored here using a simple organic matter degradation model (Supplementary Information sections 4.1 and 4.2).

Overall, the river and soil data here show how 1/[OC] and $\Delta^{14}C$ can be used to examine the role of OC_{petro} input. A domain of OC and $\Delta^{14}C$ values can most easily be reached by OC_{petro} addition to the organic matter pool (Fig. 1b), as seen in the grey "mixing zone" of sedimentary soils. In the igneous soils, this mixing domain is harder to populate. We note the importance of OC_{petro} is likely to be most relevant in soils with low OC_{bio} inputs or relatively old ^{14}C mean ages, which could be particularly important in deep soils (Rumpel and Kögel-Knabner, 2011; Shi *et al.*, 2020).

Widespread OC_{petro} input to global soils

To assess a potential, wider input of OC_{petro} into soils, we use the ISRaD database (Lawrence *et al.*, 2020) (see Supplementary Information). All database samples used have reported $\Delta^{14}C$ values and *measured* (not extrapolated or modelled) [OC] (Fig. 2a). We characterise the parent material for each geo-located profile from the global lithological map database (GLiM) (Hartmann and Moosdorf, 2012) if no parent material is specified in the database (79.4 % of entries). The soil radiocarbon profiles are split into sedimentary (SED) (80.9 %) and igneous (IG) (19.4 %) parent material, with 557 soil profiles and 2978 radiocarbon measurements (Supplementary Information) (Fig. 2e). There are more SED profiles (397 profiles, 2260 measurements) than IG profiles (160 profiles, 718 measurements), broadly mirroring the fact that ~60 % of Earth's terrestrial surface is composed of sedimentary rock (Hartmann and Moosdorf, 2012). An important caveat is that we do not capture all Quaternary deposits such

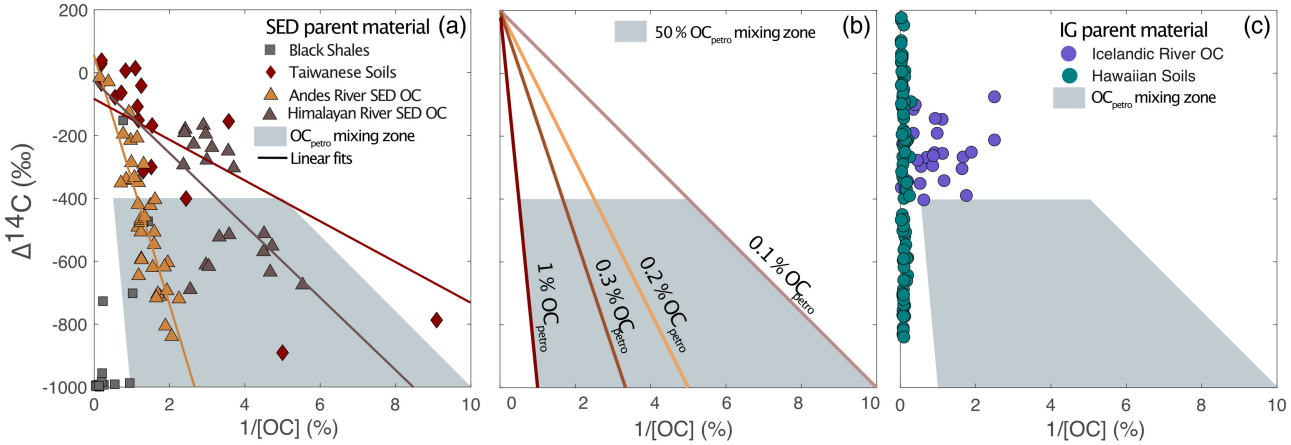

Figure 1 Rock organic carbon imprints on organic carbon concentration (OC) and radiocarbon activity ($\Delta^{14}C$). **(a)** Samples from Taiwanese soils, Andes and Himalayan rivers, and black shale weathering profiles where OC_{petro} inputs are known, with linear fits through data shown. **(b)** Binary mixing model (lines) between OC_{bio} ($\Delta^{14}C = +200$ ‰) and OC_{petro} (varying from 1 % to 0.1 % of total OC, $\Delta^{14}C = -1000$ ‰). The grey shaded area is where >50 % of total OC is OC_{petro}. **(c)** Samples where OC_{petro} is absent: soil from Hawaiian Pololu lava flow and Icelandic river samples draining basalt.

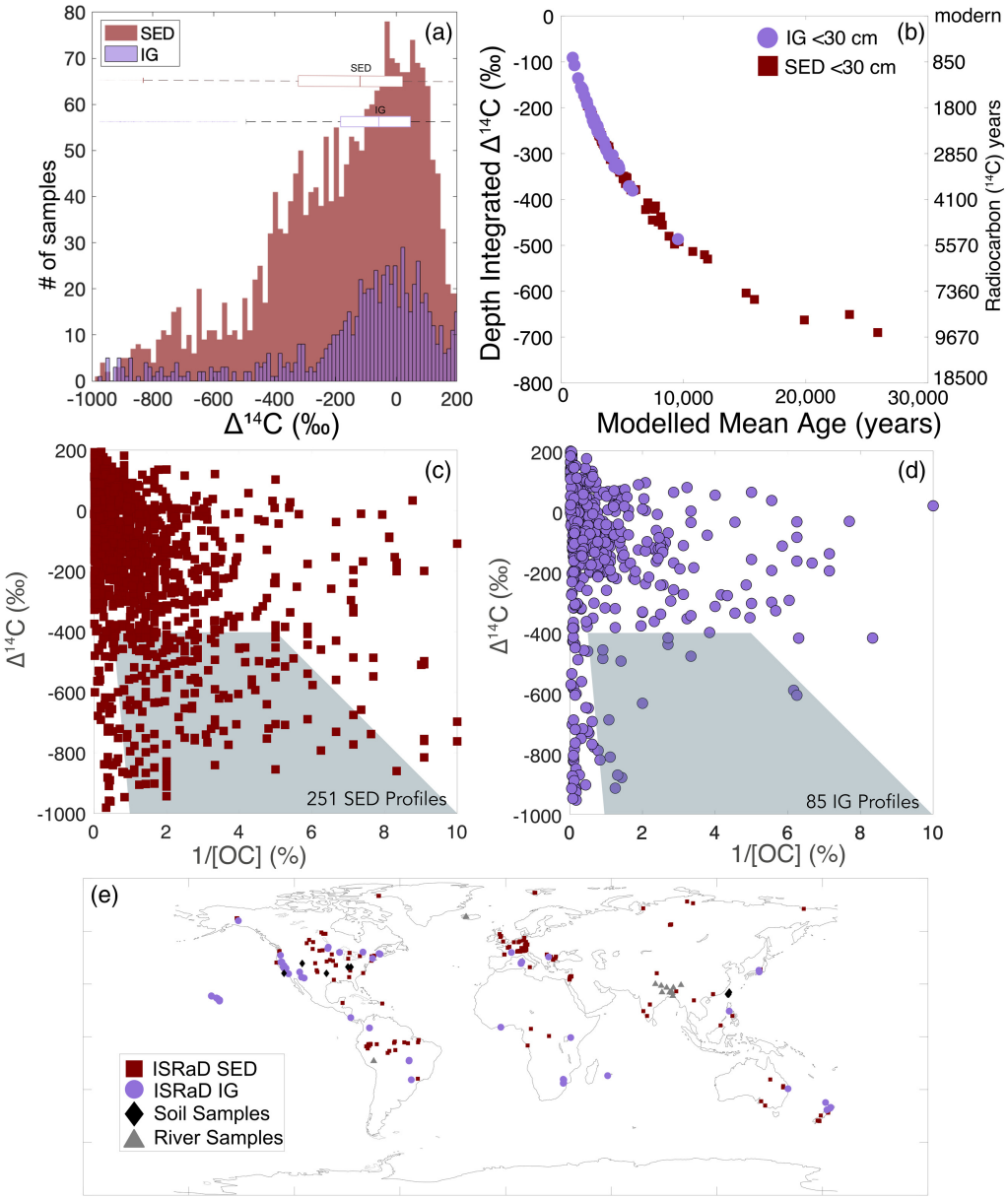

Figure 2 **(a)** The distribution of radiocarbon measurements for the SED and IG profiles, with corresponding box plots depicting the median and quartiles of the distributions. **(b)** The depth integrated $\Delta^{14}C$ (displayed in ‰ and ^{14}C years) *vs.* modelled mean ages extracted from the Shi *et al.* (2020) dataset for the SED and IG profiles. **(c)** The ISRaD soil horizons from SED soils plotted in 1/[OC] and radiocarbon ($\Delta^{14}C$). **(d)** The ISRaD soil horizons from IG soils plotted in 1/[OC] and radiocarbon activity ($\Delta^{14}C$). The grey shaded region defines a zone where mixing of OC_{petro} can produce compositions which are difficult to obtain via OC decomposition alone (Fig. 1b). **(e)** Locations of samples where direct measurement of OC_{petro} inputs have been identified (diamond, triangle), and soil profiles from the ISRaD database on igneous (IG, circles) and sedimentary rocks (SED, squares).

as loess or ashfall, which are important parent materials for soil (Baisden and Parfitt, 2007). Rather than filter the database further, we note some of the SED samples on loess or ashfall may have very low OC_{petro} inputs.

Despite the complexities inherent in any global soil assessment (Lawrence *et al.*, 2020), characterising samples from ISRaD as from either SED or IG sites reveals patterns which can be accounted for by OC_{petro} inputs. First, the median and lower quartile $\Delta^{14}C$ values of SED samples are lower than IG sites (Fig. 2c, Table S-2). Second, the distribution of SED and IG soil $\Delta^{14}C$ values are significantly different at the 0.05 level (Kolomogorov-Smirnov Test). Third, the calculated profile-averaged $\Delta^{14}C$ values and modelled mean soil age are significantly different between SED and IG profiles ($p > 0.05$, Supplementary Information section 1.3). Finally, the SED samples that reach lower $\Delta^{14}C$ values (Fig. 2c) define the grey zone suggested by a binary mixing model (Fig. 1b). IG profiles do not commonly reach this range of compositions, with the ^{14}C depleted samples either having retained higher % OC, or remain fairly ^{14}C-enriched ($\Delta^{14}C > -200$ ‰) as OC is lost, *i.e.* have a shallower trajectory between 1/[OC] and $\Delta^{14}C$ (Fig. 2d).

Having established potential OC_{petro} inputs at SED sites, the radiocarbon data can be used to quantify a maximum permissible OC_{petro} input. To do so, we assume all ^{14}C-depletion is driven by OC_{petro} addition (*i.e.* no OC_{bio} ageing) (Supplementary Information section 5.1). We calculate an average maximum proportion of $OC_{petro} = 0.38$ or 38 % (Fig. 3b) for all SED soils. This corresponds to an average 0.85 ± 0.1 % OC_{petro} in soils (Fig. 3c).

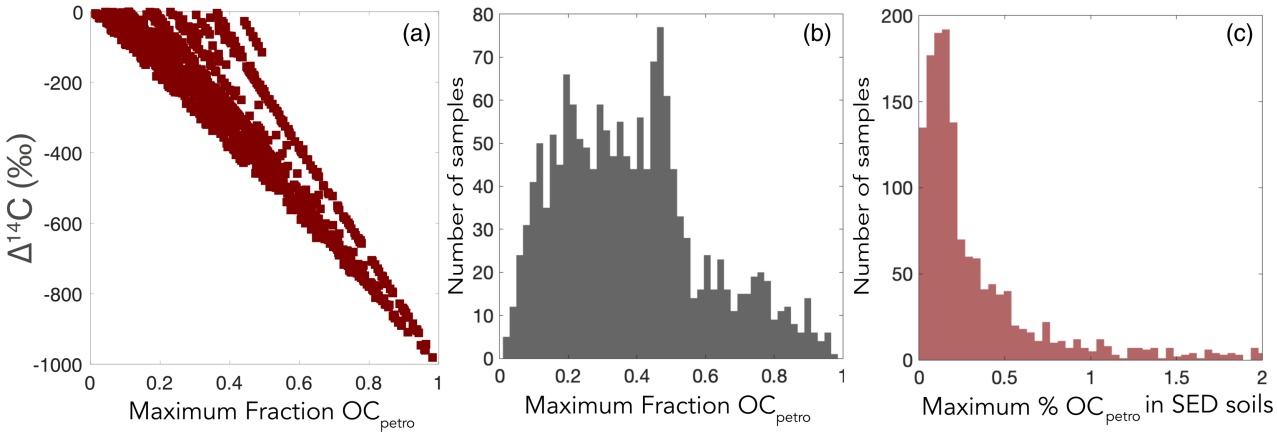

Figure 3 **(a)** The maximum fraction of [OC_{petro}] is calculated via a binary mixing model between OC_{bio} and OC_{petro} in the globally distributed soil profiles (ISRaD database). **(b)** A histogram of the maximum fraction of OC_{petro} values for each soil sample. The mean f_{petro} is 0.38 ± 0.01, the median value is 0.36. **(c)** A histogram of calculated maximum OC_{petro} (wt. %) in each SED soil horizon. The average is 0.85 ± 0.1 wt. % OC and the median is 0.19 % OC_{petro} in SED soils globally.

This maximum value is reasonable given known OC contents of sedimentary rocks (Graz *et al.*, 2011; Partin *et al.*, 2013).

Taken together, our analysis places a maximum bound on the OC_{petro} content to deep and ^{14}C depleted soils forming on sedimentary rocks. While this estimation is an upper bound because OC_{bio} ageing will occur in deep soils (Grant *et al.*, 2022), and does not consider loss of OC_{petro} during weathering, it is a reasonable starting point to understand how incorporation of OC_{petro} can influence mean soil age.

OC_{petro} in soils leads to mean age overestimation

Input of OC_{petro} in soils formed on sedimentary rocks is consistent with patterns in the dataset (Fig. 2c, d). If OC_{petro} contributes to deep soils, how much could it alter carbon residence times based on ^{14}C measurements? To provide a first constraint, we reconsider the Shi *et al.* (2020) global weighted $\Delta^{14}C$ accounting for a fraction of OC_{petro}. The mean age in subsoils (30–100 cm depth) was $\Delta^{14}C = -391 \pm 56$ ‰ (~3970 ^{14}C years). Accounting for our calculated maximum fraction of 0.38 OC_{petro} could mean the OC_{bio} age calculated in the Shi *et al.* (2020) dataset is equivalent to −17.7 ‰, or 150 ^{14}C years, a difference of ~3800 ^{14}C years. Using a more modest mass fraction of 0.10 for OC_{petro} would shift the biospheric radiocarbon age younger by 800 ^{14}C years (from 3900 to 3100 ^{14}C yr). While a 38 % OC_{petro} contribution is likely an overestimation, the analysis shows that even modest OC_{petro} inputs could shift assessments of OC_{bio} residence time in soils, yet OC_{petro} inputs are not considered in global assessments (He *et al.*, 2016; Shi *et al.*, 2020). An "apparent" increase in OC_{bio} age by failing to account for OC_{petro} addition would imply soil carbon exchange fluxes with the atmosphere are underestimated. Accounting for the fate of OC_{petro} in soils is important for reducing uncertainty on the present and future role of soils in the anthropogenic carbon budget.

The input of OC_{petro} to soils is central to the long-term carbon cycle. It is important to assess the OC_{petro} input to soils, its oxidation during soil formation that can release CO_2, and the potential influence of OC_{petro} on soil OC stabilisation mechanisms. We can compare our maximum OC_{petro} contents (Fig. 3) from the SED soil profiles from ISRaD to global sedimentary rock OC values (Fig. S-3). These sedimentary rock samples have higher OC contents than sedimentary soils, suggesting the widespread loss of OC_{petro} in global soils (Partin *et al.*, 2013). Traditionally, OC_{petro} is considered inert or unreactive on anthropogenic timescales. However, in Taiwanese soils, Hemingway *et al.* (2018) found that ~67 % of OC_{petro} was lost during soil formation, even during rapid erosion which limits time for soil weathering. This extensive OC_{petro} oxidation was attributed to microbial assimilation of OC_{petro} (Hemingway *et al.*, 2018). To move forward, we must recognise that, like OC_{bio} in soil, OC_{petro} is a continuum of compounds which differ in chemistry, linked to the history of past sedimentation, diagenesis, and metamorphism (Galy *et al.*, 2008; Petsch, 2014) which may have a distribution of reactivities and residence times in soils. Radiocarbon measurements suggest that OC_{petro} contribution to soils is a global feature and so needs to be considered to properly constrain soil carbon storage and turnover. Quantifying the fate of OC_{petro} in soils is then crucial to understanding the evolution of the long-term carbon and oxygen cycles.

Acknowledgements

This work was performed under the European Research Council (ERC) Starting Grant (678779, ROC-CO_2) and partly under an ERC Consolidator Grant (101002563, RIV-ESCAPE) to RGH. Partial writing of this work was performed under the auspices of the U.S. Department of Energy by Lawrence Livermore National Laboratory under contract DE-AC52-07NA27344 (LLNL-JRNL-837045).

Editor: Liane G. Benning

Additional Information

Supplementary Information accompanies this letter at https://www.geochemicalperspectivesletters.org/article2312.

Cite this letter as: Grant, K.E., Hilton, R.G., Galy, V.V. (2023) Global patterns of radiocarbon depletion in subsoil linked to rock-derived organic carbon. *Geochem. Persp. Let.* 25, 36–40. https://doi.org/10.7185/geochemlet.2312

References

Agnelli, A., Trumbore, S.E., Corti, G., Ugolini, F.C. (2002) The dynamics of organic matter in rock fragments in soil investigated by ^{14}C dating and measurements of ^{13}C. *European Journal of Soil Science* 53, 147–159. https://doi.org/10.1046/j.1365-2389.2002.00432.x

Baisden, W.T., Parfitt, R.L. (2007) Bomb ^{14}C enrichment indicates decadal C pool in deep soil? *Biogeochemistry* 85, 59–68. https://doi.org/10.1007/s10533-007-9101-7

Clark, K.E., Hilton, R.G., West, A.J., Robles Caceres, A., Gröcke, D.R., Marthews, T.R., Ferguson, R.I., Asner, G.P., New, M., Malhi, Y. (2017) Erosion of organic carbon from the Andes and its effects on ecosystem carbon dioxide balance. *Journal of Geophysical Research: Biogeosciences* 122, 449–469. https://doi.org/10.1002/2016JG003615

Copard, Y., Amiotte-Suchet, P., Di-Giovanni, C. (2007) Storage and release of fossil organic carbon related to weathering of sedimentary rocks. *Earth and Planetary Science Letters* 258, 345–357. https://doi.org/10.1016/j.epsl.2007.03.048

Galy, V., Beyssac, O., France-Lanord, C., Eglinton, T. (2008) Recycling of Graphite During Himalayan Erosion: A Geological Stabilization of Carbon in the Crust. *Science* 322, 943–945. https://doi.org/10.1126/science.1161408

Galy, V., Peucker-Ehrenbrink, B., Eglinton, T. (2015) Global carbon export from the terrestrial biosphere controlled by erosion. *Nature* 521, 204–207. https://doi.org/10.1038/nature14400

Grant, K.E., Galy, V.V., Haghipour, N., Eglinton, T.I., Derry, L.A. (2022) Persistence of old soil carbon under changing climate: The role of mineral-organic matter interactions. *Chemical Geology* 587, 120629. https://doi.org/10.1016/j.chemgeo.2021.120629

Graz, Y., Di-Giovanni, C., Copard, Y., Elie, M., Faure, P., Laggoun Defarge, F., Lévèque, J., Michels, R., Olivier, J.E. (2011) Occurrence of fossil organic matter in modern environments: Optical, geochemical and isotopic evidence. *Applied Geochemistry* 26, 1302–1314. https://doi.org/10.1016/j.apgeochem.2011.05.004

Hartmann, J., Moosdorf, N. (2012) The new global lithological map database GLiM: A representation of rock properties at the Earth surface. *Geochemistry, Geophysics, Geosystems* 13, Q12004. https://doi.org/10.1029/2012GC004370

He, Y., Trumbore, S.E., Torn, M.S., Harden, J.W., Vaughn, L.J.S., Allison, S.D., Randerson, J.T. (2016) Radiocarbon constraints imply reduced carbon uptake by soils during the 21st century. *Science* 353, 1419–1424. https://doi.org/10.1126/science.aad4273

Hemingway, J.D., Hilton, R.G., Hovius, N., Eglinton, T.I., Haghipour, N., Wacker, L., Chen, M.-C., Galy, V.V. (2018) Microbial oxidation of lithospheric organic carbon in rapidly eroding tropical mountain soils. *Science* 360, 209–212. https://doi.org/10.1126/science.aao6463

Hemingway, J.D., Rothman, D.H., Grant, K.E., Rosengard, S.Z., Eglinton, T.I., Derry, L.A., Galy, V.V. (2019) Mineral protection regulates long-term global preservation of natural organic carbon. *Nature* 570, 228–231. https://doi.org/10.1038/s41586-019-1280-6

Hilton, R.G., West, A.J. (2020) Mountains, erosion and the carbon cycle. *Nature Reviews Earth & Environment* 1, 284–299. https://doi.org/10.1038/s43017-020-0058-6

Hilton, R.G., Turowski, J.M., Winnick, M., Dellinger, M., Schleppi, P., Williams, K.H., Lawrence, C.R., Maher, K., West, M., Hayton, A. (2021) Concentration-Discharge Relationships of Dissolved Rhenium in Alpine Catchments Reveal Its Use as a Tracer of Oxidative Weathering. *Water Resources Research* 57, e2021WR029844. https://doi.org/10.1029/2021WR029844

Jackson, R.B., Lajtha, K., Crow, S.E., Hugelius, G., Kramer, M.G., Piñeiro, G. (2017) The Ecology of Soil Carbon: Pools, Vulnerabilities, and Biotic and Abiotic Controls. *Annual Review of Ecology, Evolution, and Systematics* 48, 419–445. https://doi.org/10.1146/annurev-ecolsys-112414-054234

Kalks, F., Noren, G., Mueller, C.W., Helfrich, M., Rethemeyer, J., Don, A. (2021) Geogenic organic carbon in terrestrial sediments and its contribution to total soil carbon. *Soil* 7, 347–362. https://doi.org/10.5194/soil-7-347-2021

Lawrence, C.R., Beem-Miller, J., Hoyt, A.M., Monroe, G., Sierra, C.A., *et al.* (2020) An open-source database for the synthesis of soil radiocarbon data: International Soil Radiocarbon Database (ISRaD) version 1.0. *Earth System Science Data* 12, 61–76. https://doi.org/10.5194/essd-12-61-2020

Mathieu, J.A., Hatté, C., Balesdent, J., Parent, É. (2015) Deep soil carbon dynamics are driven more by soil type than by climate: a worldwide meta-analysis of radiocarbon profiles. *Global Change Biology* 21, 4278–4292. https://doi.org/10.1111/gcb.13012

Partin, C.A., Bekker, A., Planavsky, N.J., Scott, C.T., Gill, B.C., Li, C., Podkovyrov, V., Maslov, A., Konhauser, K.O., Lalonde, S.V., Love, G.D., Poulton, S.W., Lyons, T.W. (2013) Large-scale fluctuations in Precambrian atmospheric and oceanic oxygen levels from the record of U in shales. *Earth and Planetary Science Letters* 369–370, 284–293. https://doi.org/10.1016/j.epsl.2013.03.031

Petsch, S.T. (2014) 12.8 - Weathering of Organic Carbon. In: Holland, H.D., Turekian, K.K. (Eds.) *Treatise on Geochemistry*. Second Edition, Elsevier, Amsterdam, 217–238. https://doi.org/10.1016/B978-0-08-095975-7.01013-5

Petsch, S.T., Eglinton, T.I., Edwards, K.J. (2001) ^{14}C-Dead Living Biomass: Evidence for Microbial Assimilation of Ancient Organic Carbon During Shale Weathering. *Science* 292, 1127–1131. https://doi.org/10.1126/science.1058332

Rumpel, C., Kögel-Knabner, I. (2011) Deep soil organic matter—a key but poorly understood component of terrestrial C cycle. *Plant and Soil* 338, 143–158. https://doi.org/10.1007/s11104-010-0391-5

Schmidt, M.W.I., Torn, M.S., Abiven, S., Dittmar, T., Guggenberger, G., Janssens, I.A., Kleber, M., Kögel-Knabner, I., Lehmann, J., Manning, D.A.C., Nannipieri, P., Rasse, D.P., Weiner, S., Trumbore, S.E. (2011) Persistence of soil organic matter as an ecosystem property. *Nature* 478, 49–56. https://doi.org/10.1038/nature10386

Shi, Z., Allison, S.D., He, Y., Levine, P.A., Hoyt, A.M., Beem-Miller, J., Zhu, Q., Wieder, W.R., Trumbore, S., Randerson, J.T. (2020) The age distribution of global soil carbon inferred from radiocarbon measurements. *Nature Geoscience* 13, 555–559. https://doi.org/10.1038/s41561-020-0596-z

Sierra, C.A., Hoyt, A.M., He, Y., Trumbore, S.E. (2018) Soil Organic Matter Persistence as a Stochastic Process: Age and Transit Time Distributions of Carbon in Soils. *Global Biogeochemical Cycles* 32, 1574–1588. https://doi.org/10.1029/2018GB005950

Torres, M.A., Kemeny, P.C., Lamb, M.P., Cole, T.L., Fischer, W.W. (2020) Long-Term Storage and Age-Biased Export of Fluvial Organic Carbon: Field Evidence From West Iceland. *Geochemistry, Geophysics, Geosystems* 21, e2019GC008632. https://doi.org/10.1029/2019GC008632

Trumbore, S. (2000) Age of Soil Organic Matter and Soil Respiration: Radiocarbon Constraints on Belowground C Dynamics. *Ecological Applications* 10, 399–411. https://doi.org/10.1890/1051-0761(2000)010[0399:AOSOMA]2.0.CO;2